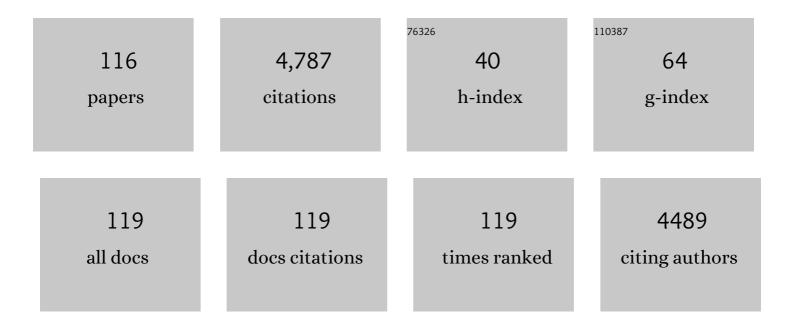
Xingbo Liu

List of Publications by Year in descending order

Source: https://exaly.com/author-pdf/1782771/publications.pdf Version: 2024-02-01



XINCRO LUI

#	Article	IF	CITATIONS
1	Sulfur-tolerant anode materials for solid oxide fuel cell application. Journal of Power Sources, 2007, 168, 289-298.	7.8	336
2	Recent Development of SOFC Metallic Interconnect. Journal of Materials Science and Technology, 2010, 26, 293-305.	10.7	300
3	Capacity Fade Analysis of Sulfur Cathodes in Lithium–Sulfur Batteries. Advanced Science, 2016, 3, 1600101.	11.2	213
4	Recent progress in Li-rich layered oxides as cathode materials for Li-ion batteries. RSC Advances, 2014, 4, 63268-63284.	3.6	167
5	Degradation of solid oxide electrolysis cells: Phenomena, mechanisms, and emerging mitigation strategies—A review. Journal of Materials Science and Technology, 2020, 55, 35-55.	10.7	133
6	Oxygen reduction and transportation mechanisms in solid oxide fuel cell cathodes. Journal of Power Sources, 2010, 195, 3345-3358.	7.8	122
7	Polyvinyl alcohol coating induced preferred crystallographic orientation in aqueous zinc battery anodes. Nano Energy, 2022, 98, 107269.	16.0	102
8	High performing triple-conductive Pr ₂ NiO _{4+δ} anode for proton-conducting steam solid oxide electrolysis cell. Journal of Materials Chemistry A, 2018, 6, 18057-18066.	10.3	101
9	The performance of solid oxide fuel cells with Mn–Co electroplated interconnect as cathode current collector. Journal of Power Sources, 2009, 189, 1106-1113.	7.8	100
10	Influence of surface modifications on pitting corrosion behavior of nickel-base alloy 718. Part 1: Effect of machine hammer peening. Corrosion Science, 2013, 77, 230-245.	6.6	94
11	DC electrodeposition of Mn–Co alloys on stainless steels for SOFC interconnect application. Journal of Power Sources, 2008, 177, 376-385.	7.8	92
12	Sulfur Immobilization by "Chemical Anchor―to Suppress the Diffusion of Polysulfides in Lithium–Sulfur Batteries. Advanced Materials Interfaces, 2018, 5, 1701274.	3.7	87
13	A review of electrophoretic deposition of metal oxides and its application in solid oxide fuel cells. Advances in Colloid and Interface Science, 2020, 276, 102102.	14.7	85
14	Pulse plating of Mn–Co alloys for SOFC interconnect applications. Electrochimica Acta, 2008, 54, 793-800.	5.2	78
15	Advanced Fuel Cell Based on New Nanocrystalline Structure Gd _{0.1} Ce _{0.9} O ₂ Electrolyte. ACS Applied Materials & Interfaces, 2019, 11, 10642-10650.	8.0	78
16	Nano-porous sulfur–polyaniline electrodes for lithium–sulfurbatteries. Nano Energy, 2015, 18, 245-252.	16.0	75
17	Engineering stable Zn-MnO2 batteries by synergistic stabilization between the carbon nanofiber core and birnessite-MnO2 nanosheets shell. Chemical Engineering Journal, 2021, 405, 126969.	12.7	74
18	High-Performance Lithium–Sulfur Batteries with a Cost-Effective Carbon Paper Electrode and High Sulfur-Loading. Chemistry of Materials, 2015, 27, 6394-6401.	6.7	73

Хіндво Liu

#	Article	IF	CITATIONS
19	Comprehensive review of chromium deposition and poisoning of solid oxide fuel cells (SOFCs) cathode materials. Renewable and Sustainable Energy Reviews, 2020, 134, 110320.	16.4	69
20	Surface Exchange and Bulk Diffusivity of LSCF as SOFC Cathode: Electrical Conductivity Relaxation and Isotope Exchange Characterizations. Journal of the Electrochemical Society, 2013, 160, F343-F350.	2.9	67
21	Charging activation and desulfurization of MnS unlock the active sites and electrochemical reactivity for Zn-ion batteries. Nano Energy, 2020, 75, 104869.	16.0	66
22	Electrophoretic deposition of (Mn,Co)3O4 spinel coating for solid oxide fuel cell interconnects. Journal of Power Sources, 2011, 196, 8041-8047.	7.8	61
23	Long-life, high-efficiency lithium/sulfur batteries from sulfurized carbon nanotube cathodes. Journal of Materials Chemistry A, 2015, 3, 10127-10133.	10.3	59
24	Synergistic Coupling of Proton Conductors BaZr _{0.1} Ce _{0.7} Y _{0.1} Yb _{0.1} O _{3â~´Î´} and La ₂ Ce ₂ O ₇ to Create Chemical Stable, Interface Active Electrolyte for Steam Electrolysis Cells. ACS Applied Materials & Interfaces, 2019, 11, 18323-18330.	8.0	57
25	Long-Life, High-Efficiency Lithium–Sulfur Battery from a Nanoassembled Cathode. Chemistry of Materials, 2015, 27, 5080-5087.	6.7	56
26	The effect of HCl in syngas on Ni–YSZ anode-supported solid oxide fuel cells. Journal of Power Sources, 2010, 195, 2149-2158.	7.8	53
27	Modeling of oxygen reduction mechanism for 3PB and 2PB pathways at solid oxide fuel cell cathode from multi-step charge transfer. Journal of Power Sources, 2012, 201, 204-218.	7.8	52
28	Influence of surface modifications on pitting corrosion behavior of nickel-base alloy 718. Part 2: Effect of aging treatment. Corrosion Science, 2014, 78, 151-161.	6.6	51
29	Liquid metal corrosion of 316L, Fe3Al, and FeCrSi in molten Zn-Al baths. Metallurgical and Materials Transactions A: Physical Metallurgy and Materials Science, 2005, 36, 2049-2058.	2.2	50
30	Effect of temperature on coal ash hot corrosion resistance of Inconel 740 superalloy. Corrosion Science, 2014, 82, 227-238.	6.6	50
31	Low-temperature water electrolysis: fundamentals, progress, and new strategies. Materials Advances, 2022, 3, 5598-5644.	5.4	50
32	Understanding of A-site deficiency in layered perovskites: promotion of dual reaction kinetics for water oxidation and oxygen reduction in protonic ceramic electrochemical cells. Journal of Materials Chemistry A, 2020, 8, 14600-14608.	10.3	48
33	A review on molten sulfate salts induced hot corrosion. Journal of Materials Science and Technology, 2021, 90, 243-254.	10.7	48
34	Nano-assembled Na2FePO4F/carbon nanotube multi-layered cathodes for Na-ion batteries. Electrochemistry Communications, 2015, 56, 46-50.	4.7	47
35	The effect of phosphine in syngas on Ni–YSZ anode-supported solid oxide fuel cells. Journal of Power Sources, 2009, 193, 739-746.	7.8	46
36	Investigation of Mn/Co coated T441 alloy as SOFC interconnect by on-cell tests. International Journal of Hydrogen Energy, 2011, 36, 4525-4529.	7.1	45

#	Article	IF	CITATIONS
37	Enhanced surface exchange activity and electrode performance of (La2â^'2xSr2x)(Ni1â^'xMnx)O4+δ cathode for intermediate temperature solid oxide fuel cells. Journal of Power Sources, 2016, 318, 178-183.	7.8	45
38	High performance La2NiO4+-infiltrated (La0.6Sr0.4)0.995Co0.2Fe0.8O3â^' cathode for solid oxide fuel cells. Journal of Power Sources, 2014, 269, 412-417.	7.8	44
39	Programmed Design of a Lithium–Sulfur Battery Cathode by Integrating Functional Units. Advanced Science, 2019, 6, 1900711.	11.2	44
40	Tolerance tests of H2S-laden biogas fuel on solid oxide fuel cells. Journal of Power Sources, 2010, 195, 4583-4592.	7.8	43
41	Studies on elements diffusion of Mn/Co coated ferritic stainless steel for solid oxide fuel cell interconnects application. International Journal of Hydrogen Energy, 2013, 38, 5075-5083.	7.1	43
42	Effect of γ′ content on the mechanical behavior of the WASPALOY alloy system. Materials Science & Engineering A: Structural Materials: Properties, Microstructure and Processing, 2001, 308, 1-8.	5.6	39
43	Oxygen Reduction Reaction Kinetics in Sr-Doped La ₂ NiO _{4+δ} Ruddlesden-Popper Phase as Cathode for Solid Oxide Fuel Cells. Journal of the Electrochemical Society, 2015, 162, F707-F712.	2.9	38
44	Effect of SO2 in flue gas on coal ash hot corrosion of Inconel 740 alloy – A high temperature electrochemical sensor study. Corrosion Science, 2013, 76, 390-402.	6.6	35
45	Electrophoretic deposition of carbon nanofibers/silicon film with honeycomb structure as integrated anode electrode for lithium-ion batteries. Electrochimica Acta, 2018, 281, 312-322.	5.2	34
46	The effect of hold-time on fatigue crack growth behaviors of WASPALOY alloy at elevated temperature. Materials Science & Engineering A: Structural Materials: Properties, Microstructure and Processing, 2003, 340, 8-14.	5.6	33
47	Corrosion fatigue crack growth behavior of oil-grade nickel-base alloy 718. Part 1: Effect of corrosive environment. Corrosion Science, 2014, 89, 146-153.	6.6	33
48	On the Formulation of a Freckling Criterion for Ni-Based Superalloy Vacuum Arc Remelting Ingots. Metallurgical and Materials Transactions A: Physical Metallurgy and Materials Science, 2010, 41, 2408-2416.	2.2	32
49	Liquid Metal Corrosion of 316L Stainless Steel, 410 Stainless Steel, and 1015 Carbon Steel in a Molten Zinc Bath. Metallurgical and Materials Transactions A: Physical Metallurgy and Materials Science, 2007, 38, 2727-2736.	2.2	31
50	Electrochemical characteristics of samaria-doped ceria infiltrated strontium-doped LaMnO3 cathodes with varied thickness for yttria-stabilized zirconia electrolytes. Journal of Power Sources, 2011, 196, 2551-2557.	7.8	31
51	Effect of Sn concentration on the corrosion resistance of Pb-Sn alloys in H2SO4 solution. Journal of Power Sources, 2006, 155, 420-427.	7.8	30
52	H2 oxidation on doped yttrium chromites/yttrium stabilized zirconia anode of solid oxide fuel cell. Journal of Power Sources, 2013, 241, 494-501.	7.8	29
53	Bifunctional 3D Hierarchical Hairy Foam toward Ultrastable Lithium/Sulfur Electrochemistry. Advanced Functional Materials, 2020, 30, 2004650.	14.9	29
54	The effect of coating crystallization and substrate impurities on magnetron sputtered doped LaCrO3 coatings for metallic solid oxide fuel cell interconnects. International Journal of Hydrogen Energy, 2009, 34, 2408-2415.	7.1	28

Xingbo Liu

#	Article	IF	CITATIONS
55	Oxygen Transport Kinetics in Infiltrated SOFCs Cathode by Electrical Conductivity Relaxation Technique. Journal of the Electrochemical Society, 2013, 160, F554-F559.	2.9	27
56	High-Entropy Perovskite as a High-Performing Chromium-Tolerant Cathode for Solid Oxide Fuel Cells. ACS Applied Materials & Interfaces, 2022, 14, 24363-24373.	8.0	27
57	Effect of thermal treatment on the fatigue crack propagation behavior of a new Ni-base superalloy. Materials Science & Engineering A: Structural Materials: Properties, Microstructure and Processing, 2008, 474, 30-38.	5.6	26
58	New mechanistic insight into the oxygen reduction reaction on Ruddlesden–Popper cathodes for intermediate-temperature solid oxide fuel cells. Physical Chemistry Chemical Physics, 2016, 18, 8502-8511.	2.8	26
59	Nanosized FeS ₂ Particles Caged in the Hollow Carbon Shell as a Robust Polysulfide Adsorbent and Redox Mediator. ACS Sustainable Chemistry and Engineering, 2020, 8, 3261-3272.	6.7	26
60	Oxidation behavior of metallic interconnects for SOFC in coal syngas. International Journal of Hydrogen Energy, 2009, 34, 1489-1496.	7.1	25
61	Simulation of Surface-Potential Driven ORR Kinetics on SOFC Cathode with Parallel Reaction Pathways. Journal of the Electrochemical Society, 2014, 161, F344-F353.	2.9	25
62	Deconvolution of Water-Splitting on the Triple-Conducting Ruddlesden–Popper-Phase Anode for Protonic Ceramic Electrolysis Cells. ACS Applied Materials & Interfaces, 2020, 12, 49574-49585.	8.0	25
63	Corrosion behavior and microstructure of electrodeposited nano-layered Ni–Cr coatings. Thin Solid Films, 2015, 595, 36-40.	1.8	24
64	An improved method to increase the predictive accuracy of the ECR technique. Solid State Ionics, 2011, 204-205, 104-110.	2.7	23
65	Evaluation of SmCo and SmCoN magnetron sputtering coatings for SOFC interconnect applications. Journal of Power Sources, 2008, 175, 833-840.	7.8	22
66	Developing TiAlN coatings for intermediate temperature solid oxide fuel cell interconnect applications. International Journal of Hydrogen Energy, 2008, 33, 189-196.	7.1	22
67	Thermodynamic assessment of liquid composition change during solidification and its effect on freckle formation in superalloys. Materials Science & Engineering A: Structural Materials: Properties, Microstructure and Processing, 2004, 386, 254-261.	5.6	21
68	Magnetron-sputtered Mn/Co(40:60) coating on ferritic stainless steel SUS430 for solid oxide fuel cell interconnect applications. International Journal of Hydrogen Energy, 2014, 39, 16061-16066.	7.1	21
69	A high-temperature mixed potential CO gas sensor for <i>in situ</i> combustion control. Journal of Materials Chemistry A, 2020, 8, 20101-20110.	10.3	21
70	Degradation of LaSr2Fe2CrO9â~Î^ solid oxide fuel cell anodes in phosphine-containing fuels. Journal of Power Sources, 2010, 195, 4013-4021.	7.8	20
71	Mixed conductive composites for â€~Low-Temperature' thermo-chemical CO ₂ splitting and syngas generation. Journal of Materials Chemistry A, 2020, 8, 13173-13182.	10.3	20
72	Positive Effects of H ₂ O on the Hydrogen Oxidation Reaction on Sr ₂ Fe _{1.5} Mo _{0.5} O _{6â^Î} -Based Perovskite Anodes for Solid Oxide Fuel Cells. ACS Catalysis, 2020, 10, 5567-5578.	11.2	20

#	Article	IF	CITATIONS
73	Redox-stable symmetrical solid oxide fuel cells with exceptionally high performance enabled by electrode/electrolyte diffuse interface. Journal of Power Sources, 2021, 488, 229458.	7.8	20
74	Investigation of the crack growth behavior of Inconel 718 by high temperature Moiré interferometry. Journal of Materials Science, 2004, 39, 1967-1973.	3.7	19
75	Characterization of Doped Yttrium Chromites as Electrodes for Solid Oxide Fuel Cell by Impedance Method. Journal of the Electrochemical Society, 2014, 161, F551-F560.	2.9	19
76	Electrophoretic Deposition of Gadoliniumâ€doped Ceria as a Barrier Layer on Yttriumâ€stabilized Zirconia Electrolyte for Solid Oxide Fuel Cells. Fuel Cells, 2017, 17, 869-874.	2.4	19
77	Intermediate-temperature solid oxide fuel cells with high performance cobalt-doped Pr0.5Ba0.5FeO3-δ anodes. Journal of Alloys and Compounds, 2018, 741, 1091-1097.	5.5	18
78	Reduced Thermal Expansion and Enhanced Redox Reversibility of La _{0.5} Sr _{1.5} Fe _{1.5} Mo _{0.5} O _{6â^îî} Anode Material for Solid Oxide Fuel Cells. ACS Applied Energy Materials, 2019, 2, 4244-4254.	5.1	18
79	Compatibility of a seal glass with (Mn,Co)3O4 coated interconnects: Effect of atmosphere. International Journal of Hydrogen Energy, 2010, 35, 7945-7956.	7.1	17
80	High temperature electrochemical sensor for in situ monitoring of hot corrosion. Corrosion Science, 2012, 65, 1-4.	6.6	17
81	Corrosion fatigue crack growth behavior of oil-grade nickel-base alloy 718. Part 2: Effect of aging treatment. Corrosion Science, 2015, 98, 280-290.	6.6	17
82	Effect of Electrical Current on Solid Oxide Fuel Cells Metallic Interconnect Oxidation in Syngas. International Journal of Applied Ceramic Technology, 2010, 7, 41-48.	2.1	16
83	On the bulk transport process and its impact on the electrode behavior of mixed conducting electrodes for SOFCs. Physical Chemistry Chemical Physics, 2017, 19, 23218-23228.	2.8	16
84	Layer-structured triple-conducting electrocatalyst for water-splitting in protonic ceramic electrolysis cells: Conductivities vs. activity. Journal of Power Sources, 2021, 495, 229764.	7.8	16
85	Protonic ceramic materials for clean and sustainable energy: advantages and challenges. International Materials Reviews, 2023, 68, 272-300.	19.3	16
86	Surface Oxygen Exchange Properties of Sr Doped La ₂ NiO _{4+δ} as SOFC Cathode: Thin-Film Electrical Conductivity Relaxation Investigation. ECS Transactions, 2015, 68, 801-808.	0.5	15
87	Chromium evaporation and oxidation characteristics of alumina-forming austenitic stainless steels for balance of plant applications in solid oxide fuel cells. International Journal of Hydrogen Energy, 2021, 46, 21619-21633.	7.1	15
88	Quenching Differential Thermal Analysis and Thermodynamic Calculation to Determine Partition Coefficients of Solute Elements in Simplified Ni-Base Superalloys. Metallurgical and Materials Transactions A: Physical Metallurgy and Materials Science, 2010, 41, 487-498.	2.2	13
89	Modeling of the oxygen reduction reaction for dense LSM thin films. Physical Chemistry Chemical Physics, 2017, 19, 30464-30472.	2.8	13
90	A study on the electrophoretic deposition of gadolinium doped ceria on polypyrrole coated yttrium stabilized zirconia. Journal of Colloid and Interface Science, 2019, 555, 115-123.	9.4	13

#	Article	IF	CITATIONS
91	In Situ Exsolved Nanoparticles on La _{0.5} Sr _{1.5} Fe _{1.5} Mo _{0.5} O _{6-<i>δ</i>} Anode Enhance the Hydrogen Oxidation Reaction in SOFCs. Journal of the Electrochemical Society, 2020, 167, 024510.	2.9	13
92	Methane Catalytic Pyrolysis by Microwave and Thermal Heating over Carbon Nanotube-Supported Catalysts: Productivity, Kinetics, and Energy Efficiency. Industrial & Engineering Chemistry Research, 2022, 61, 5080-5092.	3.7	13
93	Development of self-powered wireless high temperature electrochemical sensor for in situ corrosion monitoring of coal-fired power plant. ISA Transactions, 2015, 55, 188-194.	5.7	11
94	Surface Transport Mechanism and Bi-Pathway ORR Kinetics for Solid Oxide Fuel Cell Cathode. Journal of the Electrochemical Society, 2014, 161, F983-F990.	2.9	9
95	Reversible <i>In-Situ</i> Exsolution of Fe Catalyst in La _{0.5} Sr _{1.5} Fe _{1.5} Mo _{0.5} O _{6-δ} Anode for SOFCs. ECS Transactions, 2019, 91, 1701-1710.	0.5	9
96	Alternating Current Electrophoretic Deposition of Gadolinium Doped Ceria onto Yttrium Stabilized Zirconia: A Study of the Mechanism. ACS Applied Materials & Interfaces, 2020, 12, 11126-11134.	8.0	9
97	Investigation of LSM-YSZ Composite Cathode Performance Degradation with a Multistep Charge Transfer Model. Journal of the Electrochemical Society, 2019, 166, F448-F457.	2.9	8
98	NiO-based sensor for in situ CO monitoring above 1000°C: behavior and mechanism. Advanced Composites and Hybrid Materials, 2022, 5, 2478-2490.	21.1	8
99	A-Site Deficient La _{2-X} NiO _{4+δ} Infiltrated LSCF Cathode with Improved Performance and Stability. ECS Transactions, 2017, 78, 593-601.	0.5	7
100	Aqueous electrophoretic deposition of gadolinium doped ceria. Colloids and Surfaces A: Physicochemical and Engineering Aspects, 2019, 579, 123717.	4.7	7
101	Reactive Wetting of an Iron-Base Superalloy MSA2020 and 316L Stainless Steel by Molten Zinc-Aluminum Alloy. Metallurgical and Materials Transactions A: Physical Metallurgy and Materials Science, 2008, 39, 1382-1391.	2.2	6
102	Thermodynamic assessment of liquid composition change during solidification and its effect on freckle formation in superalloys. Materials Science & Engineering A: Structural Materials: Properties, Microstructure and Processing, 2004, 386, 254-261.	5.6	6
103	Wetting and Reaction Characteristics of Al ₂ O ₃ /SiC Composite Refractories by Molten Aluminum and Aluminum Alloy. International Journal of Applied Ceramic Technology, 2007, 4, 514-523.	2.1	5
104	Performance and stability of large planar solid oxide fuel cells using phosphine contaminated hydrogen fuel. Journal of Power Sources, 2018, 395, 185-194.	7.8	5
105	H ₂ Oxidation on Doped Yttrium Chromites Anode of Solid Oxide Fuel Cell. ECS Transactions, 2013, 57, 1479-1489.	0.5	4
106	Effect of Mg/Mo Ratio in Stoichiometric Sr ₂ MgMoO _{6-δ} (SMM) <sub />Redox-Stable Anode. ECS Transactions, 2017, 78, 1205-1215.</sub 	0.5	4
107	Improving Corrosion Resistance of Ferrous Alloy to Molten Zn by Modifying the Laves Phase Characteristics. Jom, 2018, 70, 2457-2462.	1.9	4
108	Combined Experimental and Numerical Analysis of Surface-Modified Solid Oxide Fuel Cell Cathodes. ECS Transactions, 2018, 85, 1289-1305.	0.5	4

#	Article	IF	CITATIONS
109	Surface decorations to abrupt change performance, robustness, and stability of electrodes for solid oxide cells. Journal of the American Ceramic Society, 2023, 106, 133-156.	3.8	3
110	Corrosion Behavior of Ebrite and SS430 in Coal Syngas with Loaded Current. International Journal of Applied Ceramic Technology, 2011, 8, 60-67.	2.1	2
111	A New Insight into the Oxygen Reduction Reaction on High Performance Cation-Ordered PBCO Perovskite as IT-SOFC Cathode. ECS Transactions, 2017, 78, 643-653.	0.5	2
112	Investigation of Alternative Mixed-Conducting Oxides for SOFC Anode Applications. ECS Transactions, 2017, 77, 1961-1969.	0.5	2
113	An Investigation of the Electrochemical Activity of (Ba/Sr)FeO _{3-y} Anodes. Journal of the Electrochemical Society, 2022, 169, 034525.	2.9	1
114	Energy and environmental issues in manufacturing industries. Jom, 2009, 61, 13-13.	1.9	0
115	Tolerance Tests of Co-Feeding Cl2 and H2S Impurities in Biogas on a Ni-YSZ Anode-Supported Solid Oxide Fuel Cell. , 2010, , .		0
116	Combined Experimental and Numerical Analysis of Surface-Modified Solid Oxide Fuel Cell Cathodes. ECS Meeting Abstracts, 2018, , .	0.0	0